Mem. S.A.It. Vol. 80, 678
© SAIt 2009
Memorie della

Polarization : Proving ground for methods in radiative transfer

K. N. Nagendra[1], L. S. Anusha[1], and M. Sampoorna[2]

[1] Indian Institute of Astrophysics, Koramangala, Bangalore 560 034, India
[2] Instituto de Astrofisica de Canarias, E-38205, La Laguna, Tenerife, Spain

Abstract. Polarization of solar lines arises due to illumination of radiating atom by anisotropic (limb darkened/brightened) radiation. Modelling the polarized spectra of the Sun and stars requires solution of the line radiative transfer problem in which the relevant polarizing physical mechanisms are incorporated. The purpose of this paper is to describe in what different ways the polarization state of the radiation 'complicates' the numerical methods originally designed for scalar radiative transfer. We present several interesting situations involving the solution of polarized line transfer to prove our point. They are (i) Comparison of the polarized approximate lambda iteration (PALI) methods with new approaches like Bi-conjugate gradient method that is faster, (ii) Polarized Hanle scattering line radiative transfer in random magnetic fields, (iii) Difficulties encountered in incorporating polarized partial frequency redistribution (PRD) matrices in line radiative transfer codes, (iv) Technical difficulties encountered in handling polarized specific intensity vector, some components of which are sign changing, (v) Proving that scattering polarization is indeed a boundary layer phenomenon. We provide credible benchmarks in each of the above studies. We show that any new numerical methods can be tested in the best possible way, when it is extended to include polarization state of the radiation field in line scattering.

Key words. line: formation – polarization – magnetic fields – turbulence – numerical radiative transfer – methods: techniques

1. Introduction

The radiative transfer equation (RTE) forms the basis of all efforts aimed at modelling spectral lines. In the recent three decades fast numerical methods have been developed to solve this equation. The study of polarization in lines provides more deeper insights because it is a 'measure of the anisotropy' prevailing in the atmosphere. The most common sources of anisotropy are, for example, the limb darkening and the external magnetic fields. We confine ourselves only to these two sources.

We show that inclusion of polarization tests the genuine speed and accuracy of any method in a stringent manner with respect to the corresponding method for the scalar intensity alone. We validate this assertion by taking several benchmarks.

The formulation of the standard problem of non-magnetic polarized RTE was due to Chandrasekhar (1950). The work of Stenflo & Stenholm (1976) represents one of the earliest papers on this topic. They used

Send offprint requests to: K. N. Nagendra, e-mail: knn@iiap.res.in

a 'core-saturation method' to solve the RTE. Dumont et al. (1977), Rees & Saliba (1982), and Faurobert (1987), used the standard 'Feautrier method' to solve this vector transfer equation. Nagendra (1986, 1988) used the discrete space method, based on differential form of the transfer equation. Rees (1978), and McKenna (1984) used integral equation approaches for the solution. All these methods can be grouped together as exact methods, where the solution was obtained 'non-iteratively'. Another common characteristic of these older methods is their demand for large computer memory and CPU time.

The work on modern iterative methods of solving RTE began with the seminal papers by Cannon (1973), and Olson et al. (1986), who used the concept of 'operator perturbation' for the spatial interaction matrix (the $\hat{\Lambda}$-matrix). These methods are popularly known as 'Approximate Lambda Iteration (ALI)' methods. The extension of ALI methods to polarization (non-magnetic) was by Faurobert-Scholl et al. (1997), and Trujillo Bueno & Manso Sainz (1999). In the last decade these so called PALI (P for polarized) methods have been applied to a variety of practical problems (see the reviews by Nagendra 2003; Trujillo Bueno 2003; Nagendra & Sampoorna 2009).

We further describe the methods that are devised to handle polarized RTE problems in weak magnetic fields. Historically, Chandrasekhar (1950) formulated a Fourier expansion technique to convert the 1D non-axisymmetric polarized RTE into an axisymmetric one (monochromatic case). This technique was later generalized by Faurobert-Scholl (1991), Nagendra et al. (1998), for the problem of line transfer, who applied it to the specific case of Hanle scattering.

2. Polarized line transfer in planar geometry

We consider the simple case of a two-level atom model.

2.1. Governing Equations

We start from the standard form of the RTE for the pure line case, in the presence of a weak magnetic field :

$$\mu \frac{\partial \boldsymbol{I}(\tau, x, \boldsymbol{\Omega})}{\partial \tau} = \phi(x)\,[\boldsymbol{I}(\tau, x, \boldsymbol{\Omega}) - \boldsymbol{S}(\tau, x, \boldsymbol{\Omega})]\,, \quad (1)$$

where $\boldsymbol{I} = (I, Q, U)^T$ is the Stokes vector. In this case we do not need to consider the Stokes V parameter, since it gets completely decoupled from the other three parameters (Landi Degl'Innocenti & Landolfi 2004). The corresponding Stokes source vector is given by

$$\begin{aligned}\boldsymbol{S}(\tau, x, \boldsymbol{\Omega}) &= \boldsymbol{G}(\tau) + \int \mathrm{d}x' \int \frac{\mathrm{d}\Omega'}{4\pi} g(x, x') \\ &\quad \times \hat{P}(\boldsymbol{\Omega}, \boldsymbol{\Omega}', \boldsymbol{B}) \boldsymbol{I}(\tau, x', \boldsymbol{\Omega}'). \quad (2)\end{aligned}$$

Here $\boldsymbol{G}(\tau)$ is the thermal source, $g(x, x') = R(x, x')/\phi(x)$ with $R(x, x')$ being the frequency redistribution function (neglecting polarization effects), and $\phi(x)$ being the Voigt profile function for the reduced frequency x. The polarization information is fully contained in the Hanle phase matrix $\hat{P}(\boldsymbol{\Omega}, \boldsymbol{\Omega}', \boldsymbol{B})$ (line scattering in the presence of the weak magnetic fields). $\mathrm{d}\tau = -k_{\mathrm{L}}\,\mathrm{d}z$ with k_{L} being the frequency averaged absorption coefficient. The component form of Eq. (1) is

$$\mu \frac{\partial I_i}{\partial \tau} = \phi(x)\,[I_i(\tau, x, \boldsymbol{\Omega}) - S_i(\tau, x, \boldsymbol{\Omega})]\,, \quad (3)$$

where $I_i\{i = 0, 1, 2\} = (I, Q, U)$ and $S_i\{i = 0, 1, 2\} = (S_I, S_Q, S_U)$. The source vector components can be expressed as

$$\begin{aligned}S_i(\tau, x, \boldsymbol{\Omega}) &= G_i(\tau) + \sum_{KQ} \mathcal{T}^K_Q(i, \boldsymbol{\Omega}) \quad (4) \\ &\times \sum_{Q'} \mathcal{N}^K_{QQ'}(\boldsymbol{B}) \int g(x, x')(J^K_{Q'})^*(\tau, x')\mathrm{d}x',\end{aligned}$$

with the mean irreducible tensor

$$J^K_Q(\tau, x) = \sum_{j=0}^{3} \int \mathcal{T}^K_Q(j, \boldsymbol{\Omega}) I_j(\tau, x, \boldsymbol{\Omega}) \frac{\mathrm{d}\boldsymbol{\Omega}}{4\pi}. \quad (5)$$

2.2. Decomposition in the irreducible basis

The Stokes intensity and source vectors can be decomposed using the irreducible spherical tensors defined in Frisch (2007, hereafter HF07, see also Landi Degl'Innocenti 1984). The advantage of this decomposition is that in the so called 'reduced space', Stokes source vector becomes independent of the angles ($\mathbf{\Omega}$), and the specific intensity $\boldsymbol{I}$ becomes independent of the azimuthal angle χ of the radiation field. These decompositions are

$$G_i(\tau) = \sum_{KQ} \mathcal{T}_Q^K(i, \mathbf{\Omega}) G_Q^K(\tau), \tag{6}$$

which is the thermal part of the source vector, with the only non-zero component $G_0^0(\tau)$,

$$S_i(\tau, x, \mathbf{\Omega}) = \sum_{KQ} \mathcal{T}_Q^K(i, \mathbf{\Omega}) S_Q^K(\tau, x), \tag{7}$$

which is the scattering part of the line source vector, and

$$I_i(\tau, x, \mathbf{\Omega}) = \sum_{KQ} \mathcal{T}_Q^K(i, \mathbf{\Omega}) I_Q^K(\tau, x, \mu), \tag{8}$$

which is the corresponding intensity vector. The I_Q^K and S_Q^K obey a transfer equation:

$$\mu \frac{\partial I_Q^K(\tau, x, \mu)}{\partial \tau} = \phi(x) \left[I_Q^K(\tau, x, \mu) - S_Q^K(\tau, x) \right], \tag{9}$$

where

$$S_Q^K(\tau, x) = G_Q^K(\tau) + \sum_{Q'} \mathcal{N}_{QQ'}^K(\boldsymbol{B}) \times \int g(x, x') (J_{Q'}^K)^*(\tau, x') \mathrm{d}x'. \tag{10}$$

Substituting Eq. (8) in Eq. (5) we obtain

$$(J_Q^K)^*(\tau, x) = \sum_{j=0}^{3} \sum_{K'Q'} \int (\mathcal{T}_Q^K)^*(j, \mathbf{\Omega}') \times \mathcal{T}_{Q'}^{K'}(j, \mathbf{\Omega}') I_{Q'}^{K'}(\tau, x, \mu') \frac{\mathrm{d}\mathbf{\Omega}'}{4\pi}. \tag{11}$$

The formal solution of Eq. (9) is:

$$I_Q^K(\tau, x, \mu) = I_Q^K(0, x, \mu)\, \mathrm{e}^{-\tau\phi(x)/\mu} - \int_0^\tau \mathrm{e}^{-(\tau'-\tau)\phi(x)/\mu} S_Q^K(\tau', x) \frac{\phi(x)}{\mu} \mathrm{d}\tau', \quad \mu < 0, \tag{12}$$

and

$$I_Q^K(\tau, x, \mu) = I_Q^K(T, x, \mu)\, \mathrm{e}^{-(T-\tau)\phi(x)/\mu} + \int_\tau^T \mathrm{e}^{-(\tau'-\tau)\phi(x)/\mu} S_Q^K(\tau', x) \frac{\phi(x)}{\mu} \mathrm{d}\tau', \quad \mu > 0. \tag{13}$$

The expression for the Hanle phase matrix $\hat{P}(\mathbf{\Omega}, \mathbf{\Omega}', \boldsymbol{B})$ in terms of $\mathcal{T}_Q^K$ is given by

$$\hat{P}_{ij}(\mathbf{\Omega}, \mathbf{\Omega}', \boldsymbol{B}) = \sum_{KQ} \mathcal{T}_Q^K(i, \mathbf{\Omega}) \times \sum_{Q'} \mathcal{N}_{QQ'}^K(\boldsymbol{B}) (-1)^{Q'} \mathcal{T}_{-Q'}^K(j, \mathbf{\Omega}'). \tag{14}$$

The magnetic kernel $\mathcal{N}_{QQ'}^K(\boldsymbol{B})$ is given by

$$\mathcal{N}_{QQ'}^K(\boldsymbol{B}) = \exp\,[\mathrm{i}(Q' - Q)\chi_B] \times \sum_{Q''} d_{QQ''}^K(\vartheta_B) d_{Q''Q'}^K(-\vartheta_B) X_{KQ''}(B), \tag{15}$$

where $(\vartheta_\mathrm{B}, \chi_\mathrm{B})$ is the field orientation with respect to the atmospheric normal, and $d_{MM'}^J$ are reduced rotation matrices which are listed in Landi Degl'Innocenti & Landolfi (2004). See HF07 for details on $X_{KQ}(B)$. The governing equations given in this section are fairly general, in the sense that they can be used either for complete redistribution (CRD), or scalar partial redistribution (PRD) functions of Hummer (1962). However, polarized line transfer actually requires the use of redistribution matrices, which contains inextricable coupling between polarization, frequency, and directions of incoming and outgoing photons. Difficulties encountered in handling such problems of PRD are deferred to section 5. For discussions concerning the numerical methods we assume CRD, that is $R(x, x') = \phi(x)\phi(x')$, for which the source vector $\boldsymbol{S}(\tau, x, \boldsymbol{n})$ or $S_Q^K(\tau, x)$ becomes frequency independent.

3. Preconditioned BiCG method for polarized line transfer

Here we describe the polarized Preconditioned Bi-Conjugate Gradient (Pre-BiCG) method. This is a method proposed recently by Paletou & Anterrieu (2009) for the unpolarized transfer in a planar medium. An extension of that work to the case of unpolarized

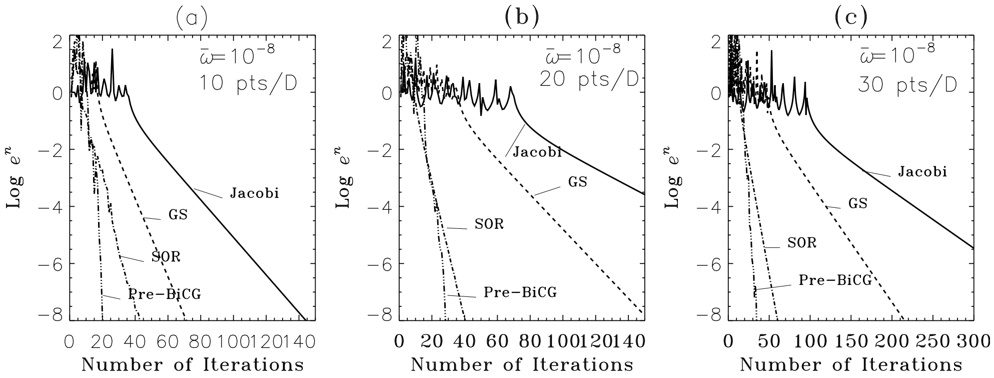

Fig. 1. Dependence of the Maximum Relative Change e^n on the iterative progress for different methods. Panels (a), (b), and (c) represent models with low, medium and high spatial resolution respectively. The model parameters are (T, a, ϵ, B_ν)= (2×10^3, 10^{-3}, 10^{-4}, 1). The convergence criteria is chosen as $\bar{\omega} = 10^{-8}$. The SOR parameter ω =1.5. The figures show clearly that Jacobi method has the smallest convergence rate, which progressively increases for GS and SOR methods. Pre-BiCG method generally has the largest convergence rate compared to the other three.

transfer in a spherical medium is described in Anusha et al. (2009) for the unpolarized case. The extension to polarization is straight forward. Therefore we do not elaborate. Here we present the convergence behaviour of this method.

Test for Convergence: Let

$$e_{\rm S} = \max_{\tau}\{|\ \delta \boldsymbol{S}/\boldsymbol{S}\ |\}, \tag{16}$$

denote the maximum relative change (MRC) on the the first component of source vector, and

$$e_{\rm P} = \max_{x,\theta,\phi}\{|\ \delta \boldsymbol{P}/\boldsymbol{P}\}\ |\ (\tau = 0), \tag{17}$$

$$\text{with} \quad P = \sqrt{(\boldsymbol{Q}/\boldsymbol{I})^2 + (\boldsymbol{U}/\boldsymbol{I})^2}, \tag{18}$$

define MRC on surface polarization. We terminate the iterative sequence when e^n =max$[e_{\rm S}, e_{\rm P}] \leq \bar{\omega}$ is satisfied, where n is the iteration number and $\bar{\omega}$ is the convergence criteria.

Figure 1 shows a plot of e^n for different methods. We can take e^n as a measure of the convergence rate. In the following we discuss how different methods respond to the grid refinement. It is a well known fact with the ALI methods, that the convergence rate is small when the resolution of the depth grid is very high. In contrast they have a high convergence rate in low resolution grids. On the other hand the Pre-BiCG method has higher convergence rate even in a high resolution grid. Figure 1a shows e^n for different methods when a low resolution spatial grid is used (10 points per decade, in the logarithmic scale for τ grid, in short 10 pts/D). The Jacobi method has the lowest convergence rate. In comparison, Gauss-Seidel (GS) method has a convergence rate which is twice that of Jacobi. The Successive Over Relaxation (SOR) method has a rate that is even better than that of GS. However Pre-BiCG has the highest convergence rate. Figure 1b and 1c are shown for intermediate (20 pts/D) and high (30 pts/D) grid resolutions. The essential point to note is that, as the grid resolution increases, the convergence rate decreases drastically and monotonically for the Jacobi and the GS methods. It is not so drastic for the SOR method. The Pre-BiCG method is relatively less sensitive to the grid resolution.

4. Polarized line transfer in random magnetic fields

Here we consider the problem of scattering in random magnetic fields. The theory of Hanle scattering in random fields was recently developed by Frisch (2006). A PALI method to solve the concerned transfer equation is developed in Frisch et al. (2009). This method is briefly described below.

In the presence of a random field of finite correlation length, Eq. (9) becomes stochastic. To solve such an equation it is necessary to represent the randomness of the field.

The random magnetic field vector $\boldsymbol{B}$ is represented by a Kubo–Anderson process (KAP). It is a stationary, discontinuous, piecewise constant, Markov process. A KAP is characterized by a correlation length $1/\nu$ (where ν is the number of jumps per unit optical depth) and a probability density function (PDF) $P(\boldsymbol{B})$. The choice of this process allows one to write a transfer equation for a mean radiation field, still conditioned by the value of $\boldsymbol{B}$ (Frisch 2006; see also Frisch et al. 2009).

In a random magnetic field the transfer equation for I^K_Q is

$$\begin{aligned}\mu\frac{\partial I^K_Q(\tau,x,\mu|\boldsymbol{B})}{\partial\tau} &= \phi(x)\Big[I^K_Q(\tau,x,\mu|\boldsymbol{B}) \\ &-S^K_Q(\tau|\boldsymbol{B})\Big] + \nu\Big[I^K_Q(\tau,x,\mu|\boldsymbol{B}) \\ &-\int I^K_Q(\tau,x,\mu|\boldsymbol{B}')P(\boldsymbol{B}')\,\mathrm{d}^3\boldsymbol{B}'\Big]. \quad (19)\end{aligned}$$

I^K_Q is now called 'conditional mean Stokes vector component' (see Frisch 2006, for its definition). Equation (19) differs from the transfer equation (9) for deterministic fields, through the last two terms (which take care of stochastic nature of the problem). The mean conditional source vector $S^K_Q(\tau|\boldsymbol{B})$ is defined by

$$\begin{aligned}S^K_Q(\tau|\boldsymbol{B}) &= G^K_Q(\tau) + \sum_{Q'}\mathcal{N}^K_{QQ'}(\boldsymbol{B}) \\ &\times\int_{-\infty}^{+\infty}\phi(x')\,(J^K_{Q'})^*(\tau,x'|\mathbf{B})\,\mathrm{d}x', \quad (20)\end{aligned}$$

where $J^K_Q(\tau,x|\mathbf{B})$ is given by Eq. (5), with I_j replaced by $I_j(\tau,x,\boldsymbol{\Omega}|\boldsymbol{B})$ which is related to $I^K_Q(\tau,x,\mu|\boldsymbol{B})$ through Eq. (8). Notice that in a random field S^K_Q explicitly depends on $\boldsymbol{B}$, in much the same way as S^K_Q depends on frequency x in PRD problems. Hence the standard numerical methods devised for PRD line transfer can be extended by simple analogy. We describe the essential steps of this method below.

The conditional source vector $\boldsymbol{\mathcal{S}}(\tau|\boldsymbol{B})$ satisfies the integral equation

$$\boldsymbol{\mathcal{S}}(\tau|\boldsymbol{B}) = \boldsymbol{\mathcal{G}}(\tau) + \hat{N}(\boldsymbol{B})\hat{\Lambda}[\boldsymbol{\mathcal{S}}], \quad (21)$$

where $\hat{N}(\boldsymbol{B})$ is the 6×6 matrix whose elements are given by Eq. (15) and $\hat{\Lambda}[\boldsymbol{\mathcal{S}}]$ and $\hat{\mathcal{L}}$ are

$$\begin{aligned}\hat{\Lambda}[\boldsymbol{\mathcal{S}}] &= \int_0^T \mathrm{d}\tau'\Big\{\hat{\mathcal{L}}(\tau-\tau';\nu)\boldsymbol{\mathcal{S}}(\tau'|\boldsymbol{B}) \\ &+[\hat{\mathcal{L}}(\tau-\tau';0)-\hat{\mathcal{L}}(\tau-\tau';\nu)] \\ &\times\int P(\boldsymbol{B}')\boldsymbol{\mathcal{S}}(\tau'|\boldsymbol{B}')\mathrm{d}^3\boldsymbol{B}'\Big\}, \quad (22)\end{aligned}$$

$$\begin{aligned}\hat{\mathcal{L}}(\tau;\nu) &= \int_{-\infty}^{+\infty}\int_0^1\frac{1}{2\mu}\,\hat{\Psi}(\mu)\,\phi^2(x) \\ &\times\exp[-|\tau|(\varphi(x)+\nu)/\mu]\,\mathrm{d}\mu\,\mathrm{d}x, \quad (23)\end{aligned}$$

where $\hat{\Psi}(\mu)$ describes the angular dependence coming from the Hanle phase matrix.

Following a standard approach we introduce an approximate $\hat{\Lambda}$ operator denoted by $\hat{\Lambda}^*$. For simplicity we consider the Jacobi scheme with $\hat{\Lambda}^*$ kept as the diagonal of non-local interaction operator $\hat{\Lambda}$. Main steps of this iteration scheme are :

$$\begin{aligned}&[\hat{E}-\hat{N}(\boldsymbol{B})\hat{\Lambda}^*]\delta\boldsymbol{\mathcal{S}}^{(n)}(\tau|\boldsymbol{B}) \\ &= \boldsymbol{\mathcal{G}}(\tau) + \hat{N}(\boldsymbol{B})\boldsymbol{\mathcal{J}}^{(n)}(\tau|\boldsymbol{B}) - \boldsymbol{\mathcal{S}}^{(n)}(\tau|\boldsymbol{B}), \quad (24)\end{aligned}$$

where $\hat{E}$ is the unit matrix and $\boldsymbol{\mathcal{J}}(\tau|\boldsymbol{B})$ is

$$\begin{aligned}\boldsymbol{\mathcal{J}}(\tau|\boldsymbol{B}) &= \int_{-\infty}^{+\infty}\frac{1}{2}\int_{-1}^{+1}\phi(x)\,\hat{\Psi}(\mu) \\ &\times\boldsymbol{\mathcal{I}}(\tau,x,\mu|\boldsymbol{B})\,\mathrm{d}\mu\,\mathrm{d}x. \quad (25)\end{aligned}$$

The source vector corrections are given by

$$\begin{aligned}\delta\boldsymbol{\mathcal{S}}^{(n)}(\tau|\boldsymbol{B}) &= \boldsymbol{\mathcal{S}}^{(n+1)}(\tau|\boldsymbol{B}) - \boldsymbol{\mathcal{S}}^{(n)}(\tau|\boldsymbol{B}); \quad (26) \\ \boldsymbol{\mathcal{J}}^{(n)}(\tau|\boldsymbol{B}) &= \hat{\Lambda}[\boldsymbol{\mathcal{S}}^{(n)}].\end{aligned}$$

The superscript (n) refers to the iteration step. Knowing $\boldsymbol{\mathcal{S}}^{(n)}(\tau|\boldsymbol{B})$, we calculate $\boldsymbol{\mathcal{J}}^{(n)}(\tau|\boldsymbol{B})$ using a formal solution of Eq. (19). A short characteristic method is used as a formal solver.

At each depth point τ_q, we have a system of linear equations for $\delta\boldsymbol{\mathcal{S}}^{(n)}(\tau_q|\boldsymbol{B})$ (see Eq. (24)).

The dimension of this system is $N_{\boldsymbol{B}} \times N_C$, with $N_C = 6$ and $N_{\boldsymbol{B}}$ the number of grid points needed to describe the PDF. If N_B, N_{ϑ_B} and N_{χ_B} are the number of grid points corresponding to strength B, inclination ϑ_B and azimuth χ_B, then $N_{\boldsymbol{B}} = N_B \times N_{\vartheta_B} \times N_{\chi_B}$. The linear system of equations for $\delta\boldsymbol{S}_j^{(n)}$ at each depth point τ_q is:

$$\sum_j \hat{A}_{ij}(\tau_q)\delta\boldsymbol{S}_j^{(n)}(\tau_q) = \boldsymbol{r}_i^{(n)}(\tau_q), \qquad (27)$$

where now $i, j = 1, \ldots, N_{\boldsymbol{B}}$. $\delta\boldsymbol{S}_j^{(n)}$ and $\boldsymbol{r}_i^{(n)}$ have the dimension N_C. We use the notation $\delta\boldsymbol{S}_j^{(n)}(\tau_q) = \delta\boldsymbol{S}^{(n)}(\tau_q|\boldsymbol{B}_j)$ with $\boldsymbol{B}_j$ the j^{th} discretized value of $\boldsymbol{B}$. Similarly, $\boldsymbol{r}_i^{(n)}(\tau_q) = \boldsymbol{r}^{(n)}(\tau_q|\boldsymbol{B}_i)$. Each element $\hat{A}_{ij}$ is an $N_C \times N_C$ block given by

$$\begin{aligned}\hat{A}_{ij}(\tau_q) \;=\; & \delta_{ij}\hat{E} - \delta_{ij}\hat{N}_i\hat{\mathcal{L}}^*(\tau_q;\nu) \\ & -\hat{N}_i[\hat{\mathcal{L}}^*(\tau_q;0) - \hat{\mathcal{L}}^*(\tau_q;\nu)]\varpi_j.\end{aligned} \qquad (28)$$

The ϖ_j are weights for the integration over magnetic field PDF. The elements $\hat{A}_{ij}$ have to be computed only once, as they do not change during the iteration cycle.

Our numerical experiments showed that, the emergent mean intensity vector (I, Q) are essentially independent of the magnetic field correlation length for optically thin ($T \ll 1$) and optically thick ($T \geq 10^3$) lines. For intermediate value of T ($10 - 100$), some sensitivity to the correlation length is exhibited. Thus in most cases of astrophysical interest, microturbulence can be safely assumed.

The mean Stokes profiles are however very sensitive to the choice of the PDF. Examples of various field strength distributions, $P(B/B_0)$ with B_0 the mean field, used in theoretical modelling of solar observations are shown in Fig. 2a. The corresponding mean Stokes $\langle Q\rangle/\langle I\rangle$ for micro-turbulent limit are shown in Fig. 2b. The angular distribution of $\boldsymbol{B}$ is assumed to be isotropic. We observe that the polarization strongly depends on the choice of $P(B/B_0)$. The sensitivity of polarization increases when PDF with large possibility for occurrence of weak fields prevail in the atmosphere (PDFs that are peaked at $B \simeq 0$).

5. Polarized line transfer with PRD

In the previous sections we assumed CRD approximation for line scattering. However a correct treatment (especially of resonance lines) requires the use of PRD. While in the scalar case it is not too difficult to handle PRD, the complexity escalates when polarized line formation is considered because PRD functions become 4×4 redistribution matrices (RMs).

In the past a "hybrid approximation" was used, which simply involves writing the RM as a product of scalar PRD function and the phase matrix that describes polarization. This has proved quite practical in the past 3 decades. See the reviews by Nagendra (2003, see also Nagendra & Sampoorna 2009) for a historical account. Note that scalar PRD function in general depends on frequencies and angles of incoming and outgoing photons, thereby making the source vectors depend not only on frequency but also on the outgoing angles (θ, φ). To overcome the (θ, φ) dependence it is a standard practice to angle average the scalar PRD functions explicitly and use them in the scattering integral (see Mihalas 1978).

The hybrid approximation worked reasonably well for non-magnetic resonance scattering. Scattering in the presence of a magnetic field (Hanle effect) calls for explicit treatment of RMs. Such RMs for arbitrary strength fields are derived recently (Bommier 1997; Bommier & Stenflo 1999; Sampoorna et al. 2007a,b), which were subsequently used in line transfer (Sampoorna et al. 2008). The difficulty in performing these computations using the full RM convinced us of the necessity to use its 'simplified forms' in practical work. One such simplification was already proposed by Bommier (1997), who derived weak field analogue of Hanle scattering RMs (both angle-averaged and angle-dependent versions). Such simplified RMs were used by Nagendra et al. (2002) in line transfer. High speed PALI method was devised to handle angle-averaged version of RMs (Fluri et al. 2003). The analysis of polarimetric data may require the use of angle-dependent RMs (exact treatment of PRD) in the line transfer computations, for which iterative methods are not yet

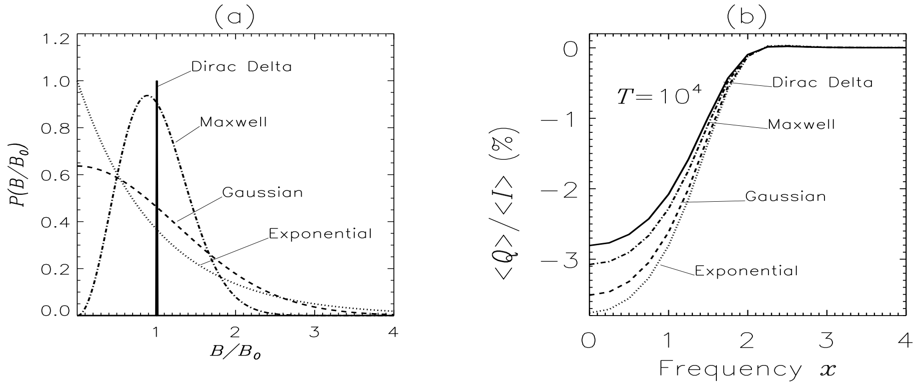

Fig. 2. Panel (a) : various $P(B/B_0)$ as a function of (B/B_0). Panel (b) : the emergent $\langle Q\rangle/\langle I\rangle$ profiles for $\mu = 0.05$, and different choice of PDFs.

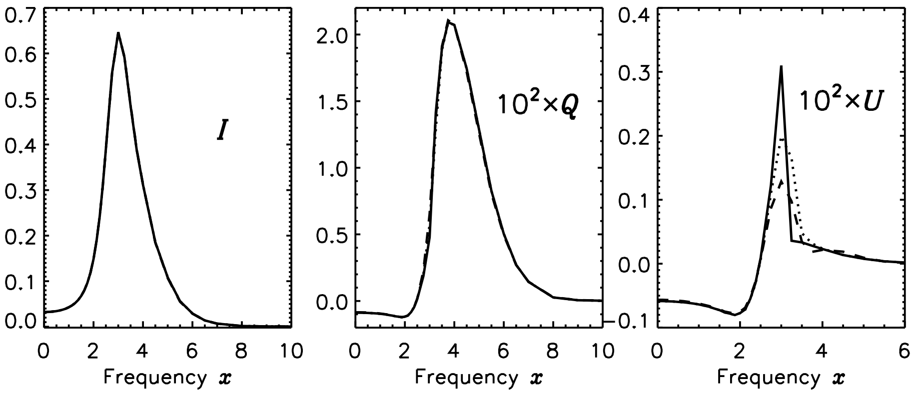

Fig. 3. Comparison of approximate treatment with the exact treatment of angle-averaged PRD. Model parameter : $(T, a, \epsilon, B_\nu) = (2 \times 10^4, 10^{-3}, 10^{-3}, 1)$. Field parameter : $(\gamma_B, \vartheta_B, \chi_B) = (1, 30°, 0°)$. Here γ_B is the Hanle efficiency factor given by $\gamma_B = eg_{\mathrm{u}}B/(2mcA_{\mathrm{ul}})$ in standard notations. Different line types : solid line (simple 1D cut-off approximation), dotted line (2D domain based cut-off approximation), and dashed line (exact treatment).

developed. Thus we are left with the dilemma of "weather to keep the exact treatment of line scattering through the use of angle-dependent RMs, or use faster iterative methods which are designed only to handle angle-averaged version of the same". The answer seems to be to develop high speed new methods of line transfer for doing angle-dependent PRD. This is a challenge for the theorist, in the near future.

Figure 3 shows a comparison of approximate versus exact treatments of angle-averaged PRD. Clearly the Stokes I and Q are insensitive to the choice of RM, while the Stokes U is considerably sensitive. We see large difference between different treatments of PRD near the cut-off frequency ($x \approx 3$) used in approximate treatments.

6. A simple grid refinement procedure in PALI

It is a well known fact that solving the polarized RTE on a fine optical depth mesh in an 'isothermal slab atmosphere' (eg. more than 10 pts/D) by PALI methods is not easy. The difficulty stems from the basic characteristic

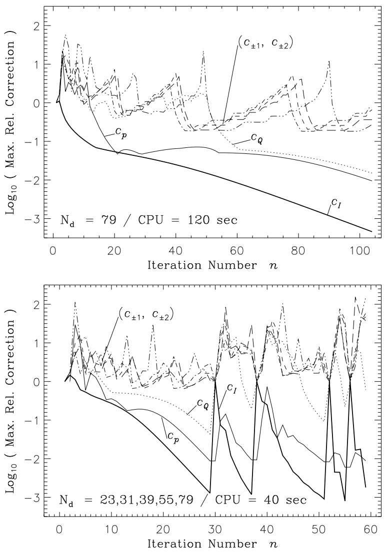

Fig. 4. The advantages of the multi-stage grid refinement procedure for solving the Hanle-PRD problem on a highly resolved spatial grid. The top panel represents the solution by a single stage PALI, using a very fine grid with 10 pts/D. The lower panel represents the solution obtained using a 5-stage grid refinement procedure. The symbols are explained in the text. The multi-stage procedure gives the solution 3 times faster than the single stage procedure.

of the polarized source vector components - namely the sign reversal as a function of optical depth $\tau-$ scale. The iterative methods compute source vector corrections in successive iterations and update the polarized source vector components using these corrections.

The MRC for the 6-component source vector and the surface polarization is

$$c_\alpha^{(n)} = \max_{\tau,x} \left\{ \frac{|\delta S_\alpha^{(n)}(\tau_k, x)|}{|\overline{S}_\alpha^{(n)}(\tau_k, x)|} \right\}, \tag{29}$$

where $k = 1, \cdots, N_d$, $\delta S_\alpha^{(n)} = |S_\alpha^{(n)} - S_\alpha^{(n-1)}|$, and $\overline{S}_\alpha^{(n)}(\tau_k, x) = 0.5 \times (|S_\alpha^{(n)}(\tau_{k-1}, x)| + |S_\alpha^{(n)}(\tau_k, x)|)$. Here α denotes $(K, Q)^{\text{th}}$ real components of S_Q^K. For example, $\alpha = I$ refers to S_0^0, $\alpha = Q$ to S_0^2, $\alpha = +1$ to $S_1^{2(x)}$, $\alpha = -1$ to $S_1^{2(y)}$, $\alpha = +2$ to $S_2^{2(x)}$, $\alpha = -2$ to $S_2^{2(y)}$, and finally $\alpha = P$ with $S_\alpha^{(n)}$ replaced by the surface polarization $\boldsymbol{P}$ refers to e_P defined in Eq. (17).

Suppose that one of the source vector component crosses zero at depth point say, k. Then in the denominator of Eq. (29), either one or both the terms $|S_\alpha^{(n)}(\tau_{k-1}, x)|$ and $|S_\alpha^{(n)}(\tau_k, x)|$ may tend to 0. If both of these terms tend 0, then $c_\alpha^{(n)} \rightarrow \infty$. In other words, these sign changes lead to the iterative correction $(\delta S/\overline{S})$ in at least one of the 5 polarized components 'growing large', instead of 'growing small', from one iteration to the next.

While this behaviour is expected in the beginning of the PALI iterative sequence, an occurrence of such a local instability after a large number of iterations, namely when we are in the smooth 'asymptotic regime of the $c_\alpha^{(n)}$ curves' is highly undesirable, as the convergence process is unnecessarily delayed. While the sign changes of $S_\alpha^{(n)}(\tau, x)$ for all α with $K = 2$, is perfectly meaningful, the spikes in the $c_\alpha^{(n)}$ curves caused actually by the denominator in Eq. (29) for all α with $K = 2$ taking very small values, do not have any physical significance. It is simply a numerical artifact, which however can delay the convergence of PALI iterative cycle. This problem is especially severe for the PRD Hanle line transfer problem in optically thick media, because there is a much larger probability of a polarization component undergoing 'zero crossing' in the (τ, x) space for high resolution in both τ and x.

Paletou & Faurobert-Scholl (1997) have proposed a simple grid refinement strategy, which they employed for the resonance line scattering problem. In this section, we have adopted the same strategy for solving a Hanle scattering PRD problem. This multi-stage grid refinement strategy performs 2 processes at each stage of $\tau-$ grid resolution :

(a) the grid doubling and searching for cross-over points (zero-crossing points), where one or more of the 6 source vector components approach zero, and remove the points on the new $\tau-$ grid which are closer to the cross-over points. This can be done by testing if

$$S_\alpha^{(n)}(\tau_{k-1}, x) S_\alpha^{(n)}(\tau_{k+1}, x) < 0. \tag{30}$$

If true, then there exists an index k' such that $S_\alpha^{(n)}(\tau_{k'}, x) \rightarrow 0$ in $[\tau_{k-1}, \tau_k]$. Moreover, if $S_\alpha^{(n)}(\tau_{k-1}, x) \rightarrow 0$, it is more likely that $S_\alpha^{(n)}(\tau_k, x)$ where τ_k is 'our chosen grid point', approaches $S_\alpha^{(n)}(\tau_{k'}, x)$. Then we encounter the problem of $c_\alpha^{(n)} \rightarrow \infty$ as explained above. To avoid this, at least one of τ_{k-1} or τ_k should be shifted to some other grid point so that the sum

$$(|S_\alpha^{(n)}(\tau_{k-1}, x)| + |S_\alpha^{(n)}(\tau_k, x)|) \nrightarrow 0. \tag{31}$$

This process of filtering the grid points often leads to a resolution less than actual doubling. (b) Interpolation of the source vector computed on the previous grid onto the new $\tau-$ grid.

Figure 4 shows the performance of this grid refinement procedure in an isothermal self-emitting slab. The model used is: $(T, a, \epsilon, B_\nu) = (200, 10^{-3}, 10^{-4}, 1)$. The magnetic field parameters are $(\gamma_B, \vartheta_B, \chi_B) = (1, 30°, 0°)$. A logarithmic frequency grid with $N_x = 25$ in the range $(0 < x < 10)$ is good enough for this optically thin case. An angle grid with $N_\mu = 5$ is used. For the test case we have presented in Fig. 4, it is possible to obtain a solution by a single stage PALI using 10 pts/D and it requires a CPU time of 120 seconds. To obtain the same solution by a 5-stage grid refinement procedure (total number of depth points at the 5 successive stages being 23, 31, 39, 55, 79), we require only 40 seconds. We note that sometimes it is impossible to obtain a solution by a single stage PALI - as the iterative sequence never converges due to the onset of too many zero-crossings of the polarized source functions. This problem is acute when we require high resolution on $\tau-$ scale, where the polarized source vector components are already close to zero in large parts of the medium (semi-infinite media with large values of thermalization parameter ϵ etc). The only alternative in such cases is to employ the multi-stage grid refinement, which provides the solution on a high resolution $\tau-$ scale, starting from quite a low resolution. This gives a reliable and accurate solution, and the final solution is obtained faster than the conventional single stage approach.

7. Practical approximations to polarized line transfer

Polarized line transfer becomes numerically more and more formidable when the physics of scattering becomes involved (to give an example, the Hanle-Zeeman RM in arbitrary fields). Thus it becomes necessary to use the concepts like (a) orders of scattering approximation, and (b) last scattering approximation in exploratory work, before embarking on the full scale problem. Here we describe these two important concepts through their practical applications.

7.1. Orders of scattering approach

In polarized line transfer this approach works as long as the degree of polarization remains small.

We start from the standard integral equation for the Hanle effect with a deterministic magnetic field, namely

$$\begin{aligned} \boldsymbol{\mathcal{S}}(\tau; \boldsymbol{B}) &= \boldsymbol{\mathcal{G}}(\tau) \\ &+ \hat{N}(\boldsymbol{B}) \int_0^T \hat{K}(\tau - \tau') \boldsymbol{\mathcal{S}}(\tau'; \boldsymbol{B})\, \mathrm{d}\tau', \end{aligned} \tag{32}$$

where the kernel $\hat{K}(\tau) = \hat{\mathcal{L}}(\tau; 0)$ (see Eq. (23)). The azimuth angle χ_B can be factored out (see Frisch et al. 2009), namely $S_Q^K = \mathrm{e}^{\mathrm{i}Q\chi_B} \mathcal{S}_Q^K$. These new components satisfy (omitting the dependence of S_Q^K on $\boldsymbol{B}$)

$$\begin{aligned} S_Q^K(\tau) &= \delta_{K0}\delta_{Q0}G(\tau) + \sum_{K'Q'} N_{QQ'}^K(\boldsymbol{B}) \\ &\times \int_0^T K_{Q'}^{KK'}(\tau - \tau') S_{Q'}^{K'}(\tau') \mathrm{d}\tau'. \end{aligned} \tag{33}$$

The notation $\boldsymbol{B}$ now stands for (B, ϑ_B), and I_Q^K satisfies the transfer equation (9), but now restricted to CRD. Clearly the equation for S_0^0 contains S_0^0 and S_0^2 only. Since, polarization is always weak for the Hanle effect, we may neglect its effect on Stokes I. We denote by

$$\begin{aligned} \tilde{S}_0^0(\tau) &= G(\tau) \\ &+ N_{00}^0 \int_0^T K_0^{00}(\tau - \tau') \tilde{S}_0^0(\tau')\, \mathrm{d}\tau', \end{aligned} \tag{34}$$

the approximate value corresponding to the exact value S_0^0. As $G(\tau) = \epsilon B_\nu$ and $N_{00}^0 = (1 - \epsilon)$, Eq. (34) takes the usual form of unpolarized integral equation for the source function.

We now replace S^0_0 by $\tilde{S}^0_0$ in the equation for S^2_Q and obtain

$$\tilde{S}^2_Q(\tau) = N^2_{Q0}(\boldsymbol{B})C^2_0(\tau) + \sum_{Q'} N^2_{QQ'}(\boldsymbol{B}) \times \int_0^T K^{22}_{Q'}(\tau-\tau')\tilde{S}^2_{Q'}(\tau')\,\mathrm{d}\tau', \quad (35)$$

where

$$C^2_0(\tau) = \int_{-\infty}^{+\infty} \frac{1}{2}\int_{-1}^{+1} \Psi^{20}_0(\mu)\,\phi(x) \times \tilde{I}^0_0(\tau,x,\mu)\,\mathrm{d}\mu\,\mathrm{d}x, \quad (36)$$

with $\Psi^{20}_0(\mu) = \frac{1}{2\sqrt{2}}(3\mu^2-1)$. The first term in Eq. (35) gives the dominant contribution that drives the polarization. Therefore Eq. (35) can be solved by the standard method of successive iterations. The zeroth order solution in this iterative scheme is the first term of Eq. (35), which is nothing but the single scattered contribution to the source vector. Neglecting the cross-coupling between the source vector components of $\tilde{S}^2_Q$ ($Q \neq Q'$) and keeping only self coupling ($Q = Q'$), we can show that $\tilde{S}^2_Q$ for the kth iterate can be 'expressed' in the form of a series :

$$[\tilde{S}^2_Q]^{(k)} = N^2_{Q0}(\boldsymbol{B})C^2_0(\tau) + \sum_{m=1}^{m=k}[\frac{7}{10}N^2_{QQ}]^m \times \int_0^T \bar{K}^{22}_Q(\tau-\tau_1)\mathrm{d}\tau_1 \int_0^T \bar{K}^{22}_Q(\tau_1-\tau_2)\mathrm{d}\tau_2 \ldots \times \int_0^T \bar{K}^{22}_Q(\tau_{k-1}-\tau_k)N^2_{Q0}(\boldsymbol{B})C^2_0(\tau_k)\,\mathrm{d}\tau_k. \quad (37)$$

Here the kernels $\bar{K}^{22}_Q = \frac{10}{7}K^{22}_Q$. From Eq. (37) we see that $[\tilde{S}^2_Q]^{(k)}$ contains contribution from all orders of scattering from $k = 0$ (single scattering) to $k+1$ times scattered photons. For optically thin and thick cases single scattering contribution is sufficient to correctly evaluate the polarization (see Fig. 5b).

In optically thin media photons suffer about one scattering and Q/I is well represented by single scattering approximation. For very thick lines, large number of scatterings do take place within the medium, but the emergent polarization is produced only by the last few scatterings which take place in a boundary layer at the top of the atmosphere. For intermediate optical thickness single scattering approximation fails (see Fig. 5a). However actual S^K_Q can be recovered by including higher orders of scattering.

In astrophysical applications we encounter resonance lines that have very large optical depths. For such lines one more level of approximation can be introduced, namely the Eddington-Barbier relation which is traditionally used for semi-infinite medium. When applied to polarization (with positive Q parallel to the solar limb) it takes the form

$$Q(0,x,\mu) \simeq -\frac{3}{2\sqrt{2}}(1-\mu^2)\tilde{S}^2_0\left(\frac{\mu}{\phi(x)}\right). \quad (38)$$

7.2. Last scattering approximation

Another practical approximation that is similar to the single scattering approximation discussed above, is the last scattering approximation (LSA). It assumes that the emergent polarization is determined by the incident radiation field anisotropy within the atmosphere where the last scattering takes place (in other words the emergent polarization is produced by the very last scattering event, rather than by multiple scattering within the atmosphere). For frequency coherent non-magnetic scattering, LSA allows us to write (Stenflo 1982)

$$\frac{Q}{I} \equiv P = W_{2,\mathrm{eff}}\, k_{\mathrm{G},\lambda}(\mu)\, k_c, \quad (39)$$

where $W_{2,\mathrm{eff}}$ is the effective atomic polarizability factor, k_c is the collisional depolarization factor, and $k_{\mathrm{G},\lambda}(\mu)$ is the anisotropy factor. $k_{\mathrm{G},\lambda}(\mu)$ is obtained by multiplying the Rayleigh phase matrix with an incident unpolarized Stokes vector $(I,\ 0,\ 0,\ 0)^{\mathrm{T}}$ and integrating over all the incoming angles. This gives (see Stenflo 1982)

$$k_{\mathrm{G},\lambda}(\mu) = \frac{(1-\mu^2)}{I_\lambda(\mu)}\frac{3}{16} \times \int_{-1}^{+1}(3\mu'^2-1)\,I_\lambda(\mu')\,\mathrm{d}\mu'. \quad (40)$$

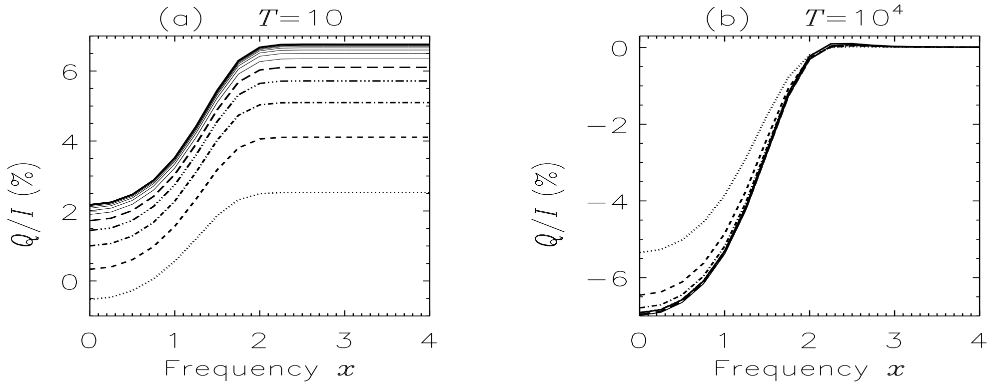

Fig. 5. Rayleigh scattering. Convergence history of the successive iteration method for the calculation of Q/I for $\tau = 0$ and $\mu = 0.05$. Different line types are : thick solid line : exact solution (from PALI); dotted : single scattering; dashed, dot-dashed, triple-dot dashed and long dashed : 2nd, 3rd, 4th, 5th and 6th iterations respectively. All the following iterations are plotted with thin solid lines.

Comparing Eq. (40) with Eq. (38) where $\tilde{S}_0^2$ is given by the single scattering approximation (i.e., $\tilde{S}_0^2 = N_{00}^2(\boldsymbol{B})C_0^2$), we see that for the particular case of 'frequency coherent scattering' (meaning in Eq. (36) we disregard integration over frequency and set $\phi(x) = 1$), $k_{G,\lambda}(\mu)$ and Q/I (of Eq. (38)) are the same.

LSA was first used by Stenflo (1982) to determine the strength of the solar micro-turbulent fields, using Hanle scattering in spectral lines. Recently Sampoorna et al. (2009) have extended the LSA concept to include the more realistic case of PRD, in the solar chromosphere, through a modelling of the Ca I 4227 Å line. The details of this method are given in Sampoorna et al. (2009, see also Sampoorna 2009, this volume).

Here we show an example of the model fits obtained using LSA. Figure 6 shows the observations done in the quite regions of the Sun, using the ZIMPOL II polarimeter at IRSOL (Locarno, Switzerland). The model profile fits the observed data very well in the wings. The near wing maxima in Q/I profiles are also fitted well. We can not expect the LSA to hold good in the line core, where the monochromatic optical depths in the profile are so large that the transfer effects can not be neglected. Therefore the line core region needs a full scale modelling using polarized line transfer.

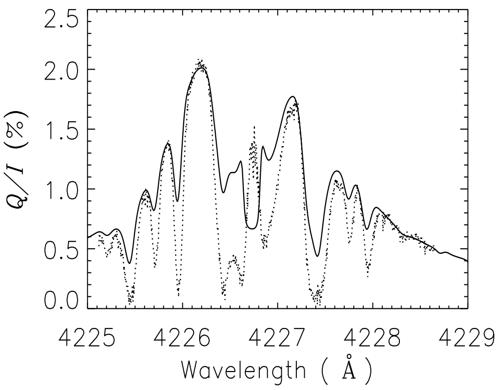

Fig. 6. Model fit obtained for collision strength $\Gamma_E/\Gamma_R = 10$ (solid line). The dotted line is the observed Q/I. Note how well the observed Q/I wings are fitted by the computed model profile.

8. Conclusions

In this paper, we show that the newly developed numerical methods of line transfer can be very well tested by applying them to solve polarized line transfer problems. We have demonstrated this through applications to benchmark problems involving physical and numerical complexity. Attention is also drawn to some peculiarities of polarized transfer.

Acknowledgements. K. N. Nagendra is grateful to the IAU for a grant, which enabled him to participate in the IAU General Assembly held at Rio de Janeiro, Brazil in 2009. He would like to thank Dr. F. Paletou for providing an unpolarized version of the grid doubling code. M. Sampoorna would like to acknowledge a grant from the IAU, which helped her to participate in the IAU General Assembly held at Rio de Janeiro, Brazil in 2009. Further she would like to acknowledge financial support by the Spanish Ministry of Science through project AYA2007-63881.

References

Anusha, L. S., Nagendra, K. N., Paletou, F., & Léger, L. 2009, ApJ, 704, 661 (arXiv: 0906.2926)

Bommier, V. 1997, A&A, 328, 726

Bommier, V., & Stenflo, J. O. 1999, A&A, 350, 327

Cannon, C. J. 1973, ApJ, 185, 621

Chandrasekhar, S. 1950, Radiative transfer, (Oxford: Clarendon Press)

Dumont, S., Pecker, J. C., Omont, A., & Rees, D. 1977, A&A, 54, 675

Faurobert, M. 1987, A&A, 178, 269

Faurobert-Scholl, M. 1991, A&A, 246, 469

Faurobert-Scholl, M., Frisch, H., & Nagendra, K. N. 1997, A&A, 322, 896

Fluri, D. M., Nagendra, K. N., & Frisch, H. 2003, A&A, 400, 303

Frisch, H. 2006, A&A, 446, 403

Frisch, H. 2007, A&A, 476, 665 (HF07)

Frisch, H., Anusha, L. S., Sampoorna, M., & Nagendra, K. N. 2009, A&A, 501, 335

Hummer, D. G. 1962, MNRAS, 125, 1

Landi Degl'Innocenti, E. 1984, Sol. Phys., 91, 1

Landi Degl'Innocenti, E., & Landolfi, M. 2004, Polarization in Spectral Lines (Kluwer Academic Publishers)

McKenna, S. J. 1984, Ap&SS, 106, 283

Mihalas, D. 1978, Stellar atmospheres (New York: 2nd Ed.; Freeman)

Nagendra, K. N. 1986, PhD Thesis (Bangalore: Bangalore Univ.)

Nagendra, K. N. 1988, ApJ, 335, 269

Nagendra, K. N. 2003, in ASP Conf. Ser. Vol. 288, Stellar Atmosphere Modelling, ed. I. Hubeny, D. Mihalas & K. Werner (San Francisco: ASP), 583

Nagendra, K. N., Frisch, H., & Faurobert-Scholl, M. 1998, A&A, 332, 610

Nagendra, K. N., Frisch, H., & Faurobert, M. 2002, A&A, 395, 305

Nagendra, K. N., & Sampoorna, M. 2009, in ASP Conf. Ser. 405, Solar Polarization 5, eds. S. V. Berdyugina, K. N. Nagendra, & R. Ramelli (San Francisco: ASP), 261

Olson, G. L., Auer, L. H., & Buchler, J. R. 1986, J. Quant. Spec. Radiat. Transf., 35, 431

Paletou, F., & Anterrieu, E. 2009, A&A, (accepted), (arXiv:0905.3258)

Paletou, F., & Faurobert-Scholl, M. 1997, A&A, 328, 343

Rees, D. E. 1978, PASJ, 30, 455

Rees, D. E., & Saliba, G. J. 1982, A&A, 115, 1

Sampoorna, M., Nagendra, K. N., & Stenflo, J. O. 2007a, ApJ, 663, 625

Sampoorna, M., Nagendra, K. N., & Stenflo, J. O. 2007b, ApJ, 670, 1485

Sampoorna, M., Nagendra, K. N., & Stenflo, J. O. 2008, ApJ, 679, 889

Sampoorna, M., Stenflo, J. O., Nagendra, K. N., Bianda, M., Ramelli, R., & Anusha, L. S. 2009, ApJ, 699, 1650

Stenflo, J. O., & Stenholm, L. 1976, A&A, 46, 69

Stenflo, J. O. 1982, Sol. Phys., 80, 209

Trujillo Bueno, J. 2003, in ASP Conf. Ser. Vol. 288, Stellar Atmosphere Modelling, ed. I. Hubeny, D. Mihalas & K. Werner (San Francisco: ASP), 551

Trujillo Bueno, J., & Manso Sainz, R. 1999, ApJ, 516, 463